

# Evidence for Stability Enhancement of Sea Ice in the Greenland and Labrador Seas

R. F. MARSDEN<sup>1</sup> AND L. A. MYSAK

*Climate Research Group, Department of Meteorology, McGill University, Montreal, Quebec, Canada*

R. A. MYERS

*Science Branch, Department of Fisheries and Oceans, St. John's, Newfoundland, Canada*

Malmberg proposed in 1969 that anomalously low surface (upper 200 m) salinities in the Iceland seas during the late 1960s could increase the stability of the water column sufficiently to prevent deep convection. The increased stability would then enhance the formation of sea ice during winter in this region because even at the freezing point ( $-1.8^{\circ}\text{C}$ ), the surface water density is sufficiently low to prevent mixing with the water below. Hence only a small portion of the water column need be cooled before freezing can occur and ice formation is enhanced. Here we explore this concept further by examining hydrographic data from three locations bordering Greenland and Iceland and then compare these with collocated sea ice concentrations. For the period 1953-1980, it is shown that the lag correlations between surface salinity and sea ice anomalies show a common structure for the case where salinity anomalies lead sea ice anomalies. It is shown that this correlation structure can be reproduced by a simple statistical feedback model using a nonstationary negative feedback coefficient to account for salinity forcing of ice anomalies. The data presented are all consistent with the concept of stability enhancement of sea ice formation.

## 1. INTRODUCTION

Fluctuations in the sea ice coverage of high-latitude oceans have profound effects on both mesoscale and global scale meteorological events. On the mesoscale, atmospheric thermal gradients near the ice edge are large, creating a location for potential storm development. At larger scales, sea ice alters the surface albedo and hence plays a critical role in the global energy balance. Finally, sea ice can hinder commercial and industrial activities in polar regions. A review of the effects of sea ice on atmospheric variability is given by Walsh [1983].

As a consequence of the increased interest in weather and climate modification by sea ice and due to the availability of large data sets, much research has focussed on the interaction between sea ice fluctuations and meteorological variables. Walsh and Johnson [1979a] show that monthly sea ice fluctuations have large spatial and long time correlation scales. Walsh and Johnson [1979b] and Johnson *et al.* [1985], however, show that the maximum correlation between sea ice fluctuations and the strongest atmospheric indicators occurs at a lag of only 1 or 2 months and that atmospheric variables incorporated into linear prediction models do not significantly increase hindcast skill over simple ice persistence (i.e., knowledge of previous ice extent). Monthly averaged atmospheric variables decorrelate over 4 to 6 months whereas ice anomalies decorrelate over periods of about 1 year, indicating a mismatch in ice and atmospheric time scales.

The effect of oceanographic variables on sea ice formation

has been examined only relatively recently. Two distinct mechanisms have been proposed to explain the oceanic effects on sea ice formation. First, poleward advection of warm ocean waters from subpolar regions is thought to play an important role in the polar heat budget and would tend to inhibit sea ice formation. Fleming [1987] showed that sea surface temperatures (SST) decorrelated at slightly longer time scales than sea ice anomalies and suggested that SST may be a good predictor of ice concentration in the Iceland Sea (East Greenland Current) region. Willmott and Mysak [1989] have presented a simple two-layer advection model driven by atmospheric heat flux and wind stress curl and have used it to obtain reasonable estimates of the climatological position of the ice edge for the Greenland and Norwegian seas. More sophisticated numerical models [e.g., Semtner, 1987] have successfully modeled the climatological seasonal ice cycle. The second mechanism involves the modulation of vertical convective processes during the winter. The major source of North Atlantic Deep water is the Greenland and Norwegian seas due to deep convective overturning [Pickard and Emery, 1982]. Malmberg [1969] proposed that in the Iceland Sea, for surface salinities of less than 34.7 psu (practical salinity units), the surface waters do not reach a high enough density even at the freezing point to sink to great depths in the water column and hence deep convection is inhibited. Warren [1983] points out that high-latitude waters in the North Atlantic have surface to bottom salinity differences of only about 0.1 psu on average and hence are preconditioned for deep convection. Conversely, the subpolar North Pacific has a mean surface to bottom salinity difference of about 2.0 psu and winter convection is limited to about 200 m. Convection then acts as an effective transport mechanism of heat from deep water to the surface. An influx of low-salinity surface water stabilizes the water column, reduces the depth of convection and promotes sea

<sup>1</sup>Now at Physics Department, Royal Roads Military College, Victoria, British Columbia, Canada.

ice formation. We will call this process stability enhancement of sea ice.

Clarke [1986] indicates that from a hydrographic survey of the Greenland Sea in 1983, while there was no direct evidence of deep convection, a numerical simulation of the region indicated that the density structure was predisposed to overturning. Rudels *et al.* [1989] show direct evidence of a deep convective plume to 1250-m depth. The deficit within the plume was about 0.2°C for temperature and 0.02 psu for salinity, while oxygen showed an excess of about 0.6 mL/L.

Oceanographic measurements are difficult to obtain at high latitudes, particularly in the winter. Thus an extensive monthly data set of hydrographic data does not exist. Malmberg [1984], however, presents tabular evidence, based on June salinities, of large sea ice concentrations off northeast Iceland being forced by surface salinity deficits. The question of time lag, though, is fundamental in examining potential sea ice forcing. One normally expects a salinity deficit to be coincident with or lag an ice excess due to ice melt. The critical question, however, is whether salinity anomalies are ever observed to lead ice anomalies to a statistically significant level. Malmberg neither calculates lag correlations nor presents arguments to show that the fluctuations have statistical significance. Mysak *et al.* [1989] show that a large negative salinity anomaly precedes a large ice anomaly by about 16 months in the Labrador Sea in 1972. Finally, Bryan [1986] on the basis of numerical model results, argues that an injection of fresh water in the south polar seas causes deep convection to be interrupted and the thermohaline circulation of the entire South Atlantic Ocean to cease. The time scale for the change was about 50 years.

In this paper, summer salinities from two locations north of Iceland and one off the Greenland coast will be examined. It will be shown that the lag correlation of the salinity fluctuations with the ice anomalies show a similar structure for each location. Furthermore, the structure is consistent with a nonstationary winter negative feedback between salinity and ice anomalies. It is suggested that the correlations are indicative of fluctuations in stability enhancement of sea ice in the adjacent polar North Atlantic seas.

The outline of the paper is as follows. In section 2 the sea ice concentrations and hydrographic data are described, and in section 3 the autocorrelations and cross correlations of the data sets are presented. A simple statistical model that simulates the sea ice–salinity cross correlations is described in section 4, and a discussion of the results is given in section 5.

## 2. DATA

Monthly sea ice concentrations from 1953 to 1984 sampled on an approximately one degree grid were obtained from J. Walsh. A synopsis of data sources and potential errors are

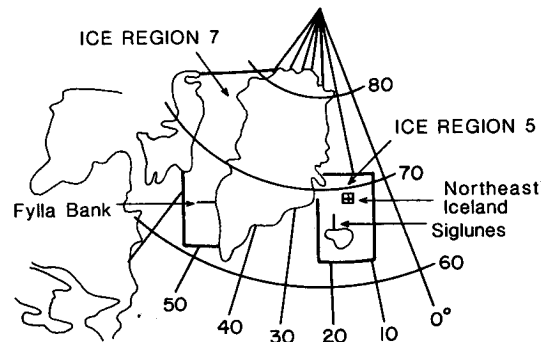


Fig. 1. Location of ice regions 5 and 7 and the hydrographic areas.

outlined by Walsh and Johnson [1979a]. The data from the North Atlantic bordering seas were grouped into eight ice regions in order to isolate areas with similar hydrographic and current structure. Furthermore, the ice climatology presented by Mysak and Manak [1989] was used as a guide to select ice areas that were neither consistently ice free nor totally iced up during any month of the year. For the eight ice regions, the ice concentrations were multiplied by surface area to arrive at the total area of ice coverage each month. The monthly means and trends for each region were calculated and subtracted from the record to yield monthly ice anomalies. Of the eight ice regions (which are used in other studies), adequate hydrographic data could be found only for regions five and seven. These regions are shown in Figure 1.

Averaged hydrographic data were obtained at the three locations shown in Figure 1. First, at Fylla Bank, located in ice region 7, the mean July salinities calculated between 50- and 150-m depth and between 400- and 600-m depth for the period 1952–1986 were obtained from Buch and Stein [1987]. The mean surface salinities (less than 50 m depth) were found to contain considerable noise from short-term runoff and precipitation and thus were not used. Second, the Siglunes section, located in ice region 5, is a series of seven oceanographic stations north of Iceland on longitude 18°50'W. We have used a weighted average of temperature and salinity from these stations over the upper 200 m from May and June calculated by J. Olafsson of the Marine Research Institute Reykjavik, Iceland. Finally, Malmberg [1984] published mean June temperature and salinity anomalies for the region 67°–69°N and 11°–15°W for the period 1950–1980. In this region, hereinafter referred to as Northeast Iceland, also in ice region 5, the data were depth averaged from 50 m to the surface. A synopsis of the hydrographic data used appears in Table 1. Next, the mean and trends were calculated and removed from all data. The

TABLE 1. Hydrographic Data Used in the Study

Region	Data Type	Depth (Average)	Month	Period
Fylla Bank	salinity	50–150 m	July	1953–1986
Fylla Bank	salinity	400–600 m	July	1953–1986
Siglunes	salinity	0–200 m	June	1952–1988
Siglunes	temperature	0–200 m	June	1952–1988
NE Iceland	salinity	0–50 m	June	1950–1980
NE Iceland	temperature	0–50 m	June	1950–1980

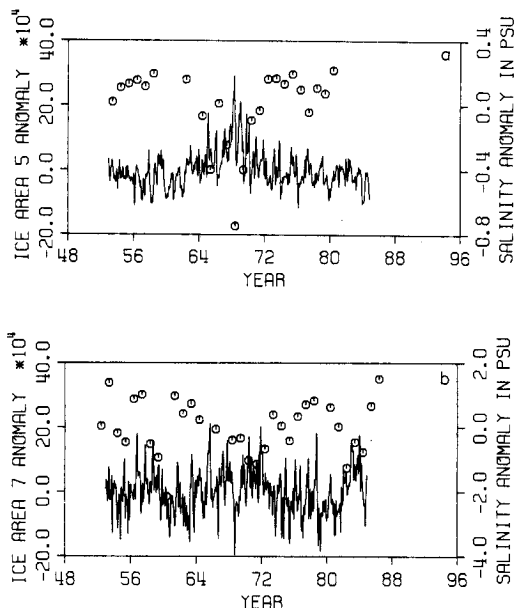


Fig. 2. Monthly time series of ice area anomalies (as a continuous line) in square kilometers and yearly near surface salinity anomalies (as octagonal symbols) for (a) ice area 5 and Northeast Iceland and (b) ice area 7 and Fylla Bank.

trends were removed to ensure that correlations were due to high-frequency fluctuations and not due to a single spurious low-frequency event. Fylla Bank and Northeast Iceland are separated by 3000 km, and the results will demonstrate the wide extent of the phenomenon. The Siglunes section and Northeast Iceland regions were used to emphasize that the same results can be obtained independent of data source and data preparation.

Figures 2a and 2b contain the monthly time series of ice area anomalies at regions 5 and 7. Superimposed are the June and July near-surface salinities at Northwest Iceland and Fylla Bank, respectively. The signal shows two characteristics. First, there is a low-frequency fluctuation in the ice anomalies of about 5 to 10 years' duration at both locations. Generally, anomalously high ice area anomalies are associated with low near-surface salinities. Second, even with the annual cycle removed (by subtracting the monthly means), there appears to be a residual signal of near annual periodicity. This suggests that summer melting is sufficient, even after periods of severe winter ice conditions, to restore the summer ice extent to near-normal conditions. To confirm this, Table 2 contains the interannual standard deviations of ice area anomalies at regions 5 and 7. There is distinct minimum in ice variability in August and September. In short, a large winter ice anomaly does not necessarily imply that a large summer ice anomaly will follow.

### 3. DATA ANALYSIS

#### 3.1. Autocorrelations

The autocorrelations for the monthly sea ice time series and the yearly salinity series are shown in Table 3. Most of the results presented in this section are similar to those obtained by Johnson *et al.* [1985]. The autocorrelation values obtained for these data will, however, be required for

TABLE 2. Standard Deviation of the Fluctuation in Ice Area Anomalies for Ice Areas 5 and 7 as a Function of Month

	Ice Area 5, $\times 10^3 \text{ km}^2$	Ice Area 7, $\times 10^3 \text{ km}^2$
January	65	80
February	70	72
March	87	58
April	66	73
May	70	53
June	50	67
July	36	80
August	23	43
September	23	41
October	32	113
November	55	98
December	65	69

subsequent analyses. The time series were modeled as autoregressive series of the form:

$$y_i = \sum_{l=1}^N a_l y_{i-l} + \eta_i \quad (1)$$

where  $y_i$  is the independent variate,  $a_l$  is an autoregressive feedback coefficient of order  $l$  and  $\eta_i$  is a noise forcing term. For the ice regions, an increase in order ( $N$ ) from 1 to 10 increased the variance covered by only 2 to 3%. Thus to a good approximation, the series can be considered to be stationary and first-order autoregressive. These results are also consistent with those of Lemke *et al.* [1980] who found the ice anomaly autospectra to fit very well to a first-order autoregressive model. The yearly salinity series at Siglunes section and Fylla Bank have similar first-order autoregression coefficients. The Siglunes section salinities were more effectively modeled as a second-order autoregressive process, while Fylla Bank and Northeast Iceland are clearly first-order autoregressive.

#### 3.2. Cross Correlations

The lag correlations were calculated between the near surface salinities, as defined in Table 3, and the sea ice. In this analysis, the yearly salinity values were compared with the corresponding monthly lead or lag of sea ice concentration. For this paper, a lag will mean that sea ice anomalies lag salinity, while a lead will mean that sea ice anomalies lead salinity. For example, when the June ice concentrations at region 7 are compared with the July salinities at Fylla Bank, the correlation would correspond to ice leading salinity by 1 month and will be referred to as a lead.

Figure 3 shows the correlation between the near-surface

TABLE 3. Autoregression Coefficients and Percent of Variance Explained at the Data Locations

Location	$a_1$	%1	%2	%10
Area 5	0.728	52.98	53.05	56.00
Area 7	0.555	30.82	31.38	33.89
Fylla Bank	0.311	12.23	15.86	...
Siglunes	0.363	13.46	21.87	...
NE Iceland	0.635	40.72	40.92	...

The % $i$  is the percent variance explained for a model of order  $i$ .

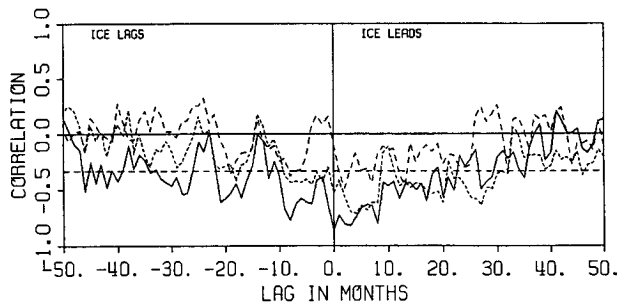


Fig. 3. Lag correlation between the near surface salinities at the three locations and the colocated ice area anomalies. The solid line is Northeast Iceland, the long-dashed line is Fylla Bank, and the short-dashed line is Siglunes Bank. The horizontal dashed line is the level below which a correlation must lie to be considered statistically different from zero to 95% confidence at Fylla Bank. The confidence limits at the other two geographic locations do not vary significantly from this value.

salinities and the local sea ice concentrations at the three locations. For ice lagging salinity, the three lag correlations are remarkably similar. First, all three series show a predominantly negative correlation. Next, all series indicate a minimum (i.e., more negative) correlation at a lag of 6 to 8 months with a second minimum at 18 to 21 months' lag. For a first-order autoregressive process, *Hannon* [1970] proposed an equivalent degrees of freedom ( $N^*$ ) as

$$N^* = N \left( \frac{1 - \rho_1 \rho_2}{1 + \rho_1 \rho_2} \right) \quad (2)$$

where  $\rho_1$  and  $\rho_2$  are the autocorrelations at lag 1 for the two series and  $N$  is the number of data points. For our analysis, the ice anomalies were sampled monthly but were compared to a yearly sampled time series of salinity. Each basis month will have a different  $N^*$  and different confidence limits. The ice anomaly autocorrelations were calculated, and it was found that 0.4 and 0.2 were typical lag 12 autocorrelations for the ice anomalies in regions 5 and 7, respectively. Table 4 shows the lag of maximum cross correlation,  $N$ ,  $N^*$ , the maximum cross correlations and the 95% confidence limits based on the  $N^*$  of equation (2). Statistically significant correlations (to 95% confidence) occur at the two minima at the three salinity regions. Finally, a bimodal structure is evident with valleys and troughs occurring at the same lags for the three locations. For ice leading salinity, the Siglunes section and Northeast Iceland data show significant negative correlations to a 30-month lag. The Fylla Bank salinities are only marginally well correlated to a 20-month lag. Possibly,

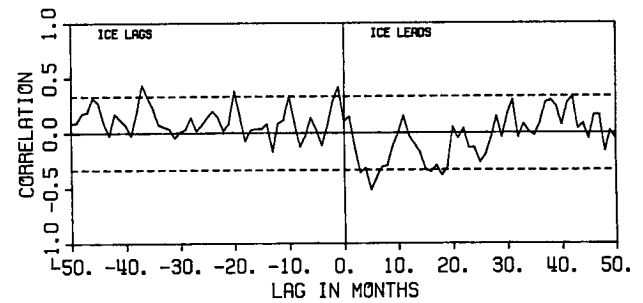


Fig. 4. Lag correlation between the 400- to 600-m-depth averaged salinity at Fylla Bank and the ice anomalies at ice region 7.

the water column at Fylla Bank is not as sensitive to stability enhancement as the Iceland Sea region of area 5. The Siglunes section curve also shows increases (i.e., less negative) in correlations to insignificant levels at 10- and 22-month leads with intervening sections of significant correlations (also see Figure 5a).

Ice formation during winter will be promoted by any salinity change that stabilizes the water column. An influx of more saline water at depth will serve the same purpose as an injection of a salinity deficit at the surface. Thus for sea ice lagging salinity, one expects a negative correlation in the near-surface layer. Deeper in the water column, the correlations should become less negative. At depth, an influx of more saline water should promote ice formation and one expects the correlations to be positive. Figure 4 shows the lag correlations of 400- to 600-m salinity with surface ice anomalies at Fylla Bank. For ice lagging salinity, the change from Figure 3 is striking. The correlations are small and on average positive, again in agreement with the concept of stability enhancement. For ice leading salinity the correlations are on average negative with significant correlations at 5 and 17 months, as one would expect for the mixing of surface ice melt into deep waters.

Figure 5a shows the correlation between the temperature and the sea ice anomaly at Siglunes section. Here the salinity and temperature time series are quite highly correlated, which is reflected in the similarity in the lag correlations. A decrease in surface salinity leads to increased surface cooling and hence a decrease in SST. Again, the curves show the oscillations as indicated in Figure 3. Overall, for ice lagging temperature and salinity, the temperature-ice correlation appears to be slightly stronger than the salinity-ice. This is not surprising, since the water temperature actually contributes to the heat budget while the salinity acts only indirectly to modulate the heat budget. In Figure 5b the temperature

TABLE 4. Estimated Confidence Limits for the Three Regions at the Correlation Minimum

Location	Lag	$N$	$N^*$	Correlation	95% Confidence
Fylla Bank	-8	32	29	-0.40	-0.37
	-19	31	28	-0.38	-0.37
Siglunes	-4	32	24	-0.46	-0.40
	-18	32	24	-0.43	-0.40
NE Iceland	-8	24	14	-0.61	-0.52
	-21	24	14	-0.77	-0.52

Lag refers to the lag of most negative correlation for the two valleys described in the text,  $N$  is the number of data points,  $N^*$  is the estimated degrees of freedom, and the rightmost column is the estimated 95% confidence zone for zero correlation based on  $N^*$  degrees of freedom.

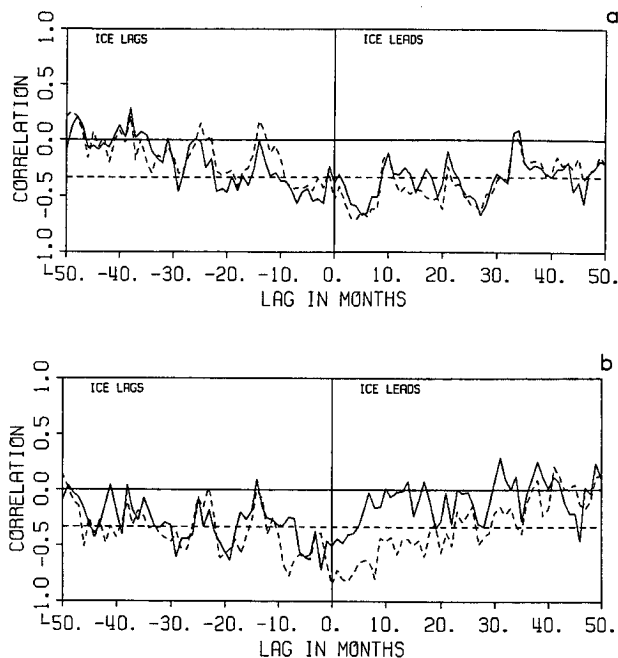


Fig. 5. Lag correlation between the 50-m temperatures and salinities at (a) Siglunes Bank and (b) Northeast Iceland and the ice area anomalies at ice region 5. The solid line is the temperature-ice correlation, while the dashed line is the salinity-ice correlation.

and salinities at Northeast Iceland are compared with the ice anomalies. Here the temperature time series is less well correlated with the salinity time series and there is less similarity in the correlation curves. There is clearly an indication of correlation minima for both temperature and salinity at 18- and 30-month lags. The curve of ice leading temperature, however, decorrelates very quickly with no significant correlation for lags greater than 8 months. Overall, the salinity appears to be more negatively correlated with ice fluctuations than is the temperature. The correlation scale decays much more rapidly for ice leading temperature than for salinity. The difference in the two results may be attributed to the fact that the Siglunes section data consist of measurements averaged between 200 m and the surface while the Northeast Iceland data have been averaged between 50 m and the surface and will include more surface meteorological influences on the temperature.

#### 4. STATISTICAL MODEL

In the preceding section it was shown that the surface salinities, and to a lesser degree the surface temperatures, show an oscillation in the lag correlation curves. Minima (i.e., strong negative correlations) occur at lags of 6, 18, and 30 months with intervening maxima. Since the series were sampled during June or July, the lags indicate that the effect of negative salinity and temperature anomalies on ice concentration would be felt most strongly the following January or February. This is in agreement with Figure 2 and Table 2, where it is suggested that summer ice concentrations are much less variable than winter concentrations possible because summer temperatures are sufficient to melt most of the previous ice excess. If stability enhancement is operative, one expects its effects to be felt most strongly in winter. During the summer the water column is stable owing to ice

melt, and the expected forcing of sea ice concentrations would be due to surface air and sea surface temperatures, independent of deep convection. In order to investigate the inherent nonstationarity of the effects of salinity on ice formation, the following statistical model was tested:

$$I_i = aI_{i-1} + b_iS_i + n_i \quad (3a)$$

$$S_i = cS_{i-1} + dI_i + m_i \quad (3b)$$

Here  $I_i$  represents surface ice concentration at month  $i$ ,  $S_i$  represents surface salinity at month  $i$ ,  $a$  and  $c$  are stationary autoregressive feedback coefficients,  $d$  is a stationary transfer function of ice forcing salinity,  $b_i$  is a nonstationary feedback coefficient, and  $n_i$  and  $m_i$  are white noise forcing functions representing processes that are uncorrelated with the salinity-ice forcing functions (e.g., fluctuations in ice advection and wind stress). The form of the nonstationary salinity transfer function is given by

For months 1–3 and 10–12

$$b_i = b_0$$

For months 4–9

$$b_i = 0.0$$

The form of  $b_i$  was chosen so that the mechanism of stability enhancement of sea ice formation was operative only during the winter months and the division of the ice year was determined from graphs of seasonal sea ice extent given by Mysak and Manak [1989]. Since salinity was sampled only once a year in all regions and the model required monthly values, the terms of the regression model could not be determined from the data. On the basis of the autocorrelation values in Table 3,  $a$  was set equal to 0.6. Using the yearly autocorrelation values of Table 3 for the salinities and assuming that the underlying series is first-order autoregressive, an estimate of the monthly autoregressive coefficient based on the yearly autocorrelation coefficient is

$$a_1 = {}^{12}\sqrt{\rho(12)}$$

Estimates of the monthly autocorrelation of salinity are in excess of 0.95 for Northeast Iceland and Siglunes section. Thus a value of 0.9 was selected for the feedback coefficient  $c$ . In running the model, it was found that the correlation at zero lag showed little fluctuation. Hence  $b_0$  and  $d$  were set to  $-0.3$  and  $-0.2$  because these values accurately reproduced the correlation coefficient for zero lag at Northeast Iceland. Although the results shown are applicable to Northeast Iceland, a similar procedure accurately reproduced the correlation structure at the two other hydrographic locations. The model was run by calculating a Gaussian random variate of unit variance for  $n_i$  and  $m_i$  at each time step. The autocorrelation portion of the model was calculated from the previous salinity and ice concentrations and the new values were determined from equation (3).

Priestley [1981, p. 119] shows that the second-order statistics of first-order autoregressive processes are asymptotically stationary and proportional to

$$(1 - a^{2t})$$

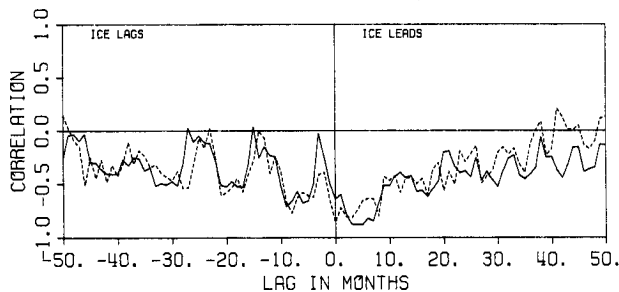


Fig. 6. Lag correlation for a selected model simulation as described in the text and between the surface salinity at Northeast Iceland and the ice area anomalies at region 5. The solid line is the simulation result, while the dashed line is the measured salinity correlation.

where  $a$  is the first-order autoregression coefficient and  $t$  is the time increment from model initialization. Consequently, the model was spun up for 500 years to ensure that the initial conditions were no longer influencing the results. The model analysis then mimicked the data analysis by calculating the lag correlations between June and the other months and the model results were compared with data correlations at Northeast Iceland. A typical 32-year realization is shown as the solid line in Figure 6. The resemblance to the oscillations in Figure 3 is striking. For ice lagging salinity, the simulated maximum at 3 months is more pronounced than that for the observed case at Northeast Iceland. However, the observed minima at 6, 18, and 30 months are well reproduced. There appears to be a mismatch at the third maximum, which appears at about 24 months in the data and at 28 months in the simulation. For ice leading salinity, the overall shape of the two curves is quite similar. It was not difficult to obtain a realization which resembled the Northeast Iceland correlation structure. For the first 10 runs, six showed the distinctive oscillatory pattern presented here. Furthermore, the model was verified with 10 different initial seeds to the random number generator with similar results achieved each time. The model was then run for 500 realizations of 32 years each. The mean and standard deviations of the lag correlations were calculated and the results appear in Figure 7a. For ice lagging salinity, the mean results are similar to the selected simulation and the data results discussed previously. For ice leading salinity, the mean patterns show a sequence of less prominent oscillations at ice leads of 10 and 22 months than occur for the ice lag correlations. There is an indication of these ice lead oscillations in the near surface Siglunes section correlations (Figure 5a) and in the Fylla Bank 400- to 600-m salinity correlations of Figure 4. These are probably due to the large autocorrelation of the two series. A large salinity minimum one summer would force excess ice the following winter, which in turn forces a salinity deficit the next summer; this is reflected in the correlations by the oscillatory pattern. The 500 simulations were then repeated using January as a basis month and are presented in Figure 7b. This is equivalent to considering June as a basis but with the transfer coefficient  $b = b_0$  during the summer and  $b = 0.0$  during the winter. The oscillations in the salinity are now completely out of phase with the June simulations and the data, indicating that oscillations observed in the data are due to a process operative in the winter.

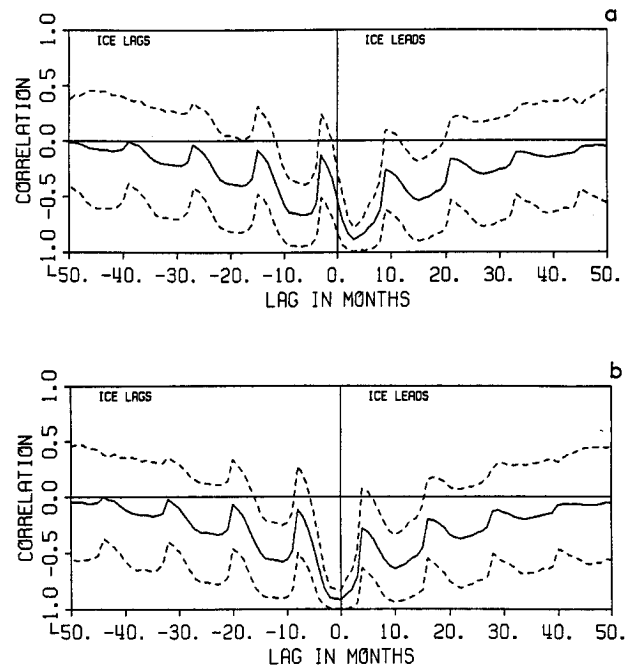


Fig. 7. Mean and  $\pm 2$  standard deviations for the model correlation results based on 500 realizations using (a) June and (b) January as a basis month.

The model reproduced the dominant oscillatory pattern for ice leading salinity only if  $b_i$  was nonstationary. When  $d$  was made nonstationary and  $b_i$  held stationary, an oscillatory pattern was produced for ice lagging salinity. If both  $b$  and  $d$  were made nonstationary, the model produced zero correlations. It was not the purpose of this simple model to attempt to describe all possible interactions that could lead to sea ice variability. Rather, we wish to show that a very simple nonstationary salinity–sea ice feedback mechanism can account for the observed correlation structure and that the structure was consistent with a winter only forcing of sea ice.

## 5. DISCUSSION AND CONCLUSIONS

The possible interruption of deep convective processes in the North Atlantic due to an influx of low-salinity surface water and subsequent stability enhancement of sea ice can have profound effects on climate. First, the heat content per unit area of a fluid is given by

$$H_s = C_p \rho T D$$

where  $C_p$  is the heat capacity at constant pressure,  $\rho$  is the density of the fluid,  $T$  is the temperature, and  $D$  is the fluid depth.  $C_p$  is approximately 4 times and  $\rho$  is 1000 times greater for water than air. Rudels *et al.* [1989] monitored a deep convection event in the Greenland Sea. Their Figure 2 indicates that the plume extended from 500-m to 1250-m depth with a mean temperature difference of about 0.2°C. This implies that  $6.5 \times 10^8 \text{ J m}^{-2}$  were released to the atmosphere. This is equivalent to heating a similar area of the atmosphere from the sea surface to the tropopause (taken to be 11 km) by 45°C. Clearly this estimate ignores (among others factors) horizontal advection by both the atmosphere and ocean and the latent heat of fusion of sea

ice, but it does serve to underline the tremendous heat capacity that would not be available to the atmosphere should the water column become more stable. Second, Whitehead [1989] gives an estimate of 1 to 5 Sv ( $1 \text{ Sv} = 10^6 \text{ m}^3 \text{ s}^{-1}$ ) for the transport over the Denmark Strait that is driven by deep convection. Aagaard [1970] gives an estimate of 10 to 20 Sv (with a maximum of 40 Sv) for the wind-driven component of the flow in the Greenland-Iceland Sea during February 1965. Deep convection can account for a significant component of the mass balance of the basin. One expects an outflow at depth to be matched by an inflow of warm surface from the south. Thus, interruption of deep convection could also have a profound effect on the northward transport of warm Atlantic surface water into the basin.

Virtually all of the data presented are consistent with stability enhancement of sea ice occurring in regions of the Greenland and Labrador seas bordering the Greenland coast. First, the surface salinities and sea ice anomalies from the three locations show significant correlation with salinity deficits leading positive sea ice anomalies. Thus anomalously large freshwater influxes are followed by increases in ice concentration. Next, the three regions, one of which (Fylla Bank) is separated from the other two by about 3000 km, show similar oscillations in the lag correlation curves. These oscillations were shown to be consistent with a nonstationary statistical feedback model where the salinity forcing was active only during the winter months: precisely the response one expects from stability enhancement. The sea ice anomalies at depth at Fylla Bank did not significantly lag the salinity anomalies, except at 2, 10, and 20 months where the salinity anomalies and sea ice anomalies were positively correlated. An influx of saline water at 400- to 500-m depth would stratify the water column and hence promote surface ice formation, which would explain a positive correlation. Finally, the 50-m temperature-ice correlations at both Siglunes section and Northeast Iceland show some indication of a similar oscillation as the salinity-ice correlation curves. The water temperature should have a direct year-round effect on sea ice by promoting or inhibiting ice formation; however, stability enhancement due to surface salinity deficits increases the effect. The results imply that deep convection has a profound effect in determining the effect of ocean temperature and salinity on sea ice production and should be taken into consideration for input to both numerical and statistical prediction models.

*Acknowledgments.* This work was completed while R.F.M. was a sabbatical visitor at McGill University. He gratefully acknowledges the support received there and from RRMCA ARP award RR15. L.A.M. gratefully acknowledges the support of NSERC, FCAR and the U.S. Office of Naval Research, code 1122ML, for this work.

## REFERENCES

- Aagaard, K., Wind-driven transports in the Greenland and Norwegian seas, *Deep Sea Res.*, 17(2), 281–291, 1970.
- Buch, E., and M. Stein, Time series of temperature and salinity at the Fylla Bank section, West Greenland, *ICES CM 1987/C:4*, 22 pp., Int. Council for the Explor. of the Sea, Copenhagen, 1987.
- Bryan, F., High-latitude salinity effects and interhemispheric thermohaline circulations, *Nature*, 323(6086), 301–304, 1986.
- Clarke, R. A., The formation Greenland Sea deep water, *ICES CM 1986/C:2*, 13 pp., Int. Council for the Explor. of the Sea, Copenhagen, 1986.
- Fleming, G. H., Predictability of Ice Concentration in the high-latitude North Atlantic from statistical analysis of SST and ice concentration data, MSc. thesis, 137 pp., Nav. Postgrad. School, Monterey, Calif., 1987.
- Hannon, E. J., *Multiple Time Series*, 424 pp., John Wiley, New York, 1970.
- Johnson, C. M., P. Lemke, and T. P. Barnett, Linear prediction of sea ice anomalies, *J. Geophys. Res.*, 90, 5665–5675, 1985.
- Lemke, P., E. W. Trinkl, and K. Hasselmann, Stochastic dynamic analysis of polar sea ice variability, *J. Phys. Oceanogr.*, 10, 2100–2120, 1980.
- Malmberg, S.-A., Hydrographic changes in the waters between Iceland and Jan Mayen in the last decade, *Joekull*, 19, 30–43, 1969.
- Malmberg, S. A., Hydrographic conditions in the East Icelandic Current and sea ice in North Icelandic waters, 1970–1980, *Rapp P. V. Reun. Counc. Int. Explor. Mer.*, 185, 170–178, 1984.
- Mysak, L. A., and D. K. Manak, Arctic sea-ice extend and anomalies, 1953–1984, *Atmos. Ocean*, 27, 376–405, 1989.
- Mysak, L. A., D. K. Mysak, and R. F. Marsden, Sea ice anomalies observed in the Greenland and Labrador Seas during 1901–1984 and their relation to an interdecadal Arctic climate cycle, *Clim. Dyn.*, in press, 1989.
- Priestly, M. B., *Spectral Analysis and Time Series*, 890 pp., Academic, San Diego, Calif., 1981.
- Pickard, G. L., and W. J. Emery, *Descriptive Physical Oceanography*, 4th ed., 249 pp., Pergamon, New York, 1982.
- Rudels, B., D. Quadfasel, H. Friedrich, and M.-N. Houssais, Greenland Sea convection in the winter of 1987–1988, *J. Geophys. Res.*, 94, 3223–3227, 1989.
- Semtner, A. J., A numerical study of sea ice and ocean circulation in the Arctic, *J. Phys. Oceanogr.*, 17, 1077–1099, 1987.
- Walsh, J. E., The role of sea ice in climatic variability: Theories and evidence, *Atmos. Ocean*, 21, 229–242, 1983.
- Walsh, J. E., and C. M. Johnson, An analysis of Arctic sea ice fluctuations, 1953–1977, *J. Phys. Oceanogr.*, 9, 580–591, 1979a.
- Walsh, J. E., and C. M. Johnson, Interannual atmospheric variability and associated fluctuations in Arctic sea ice extent, *J. Geophys. Res.*, 84, 6915–6928, 1979b.
- Warren, B. A., Why is no deep water formed in the North Pacific?, *J. Mar. Res.*, 41, 327–347, 1983.
- Whitehead, J. A., Giant ocean cataracts, *Sci. Am.*, 260(2), 50–57, 1989.
- Willmott, A. J., and L. A. Mysak, A simple steady-state coupled ice-ocean model, with application to the Greenland-Norwegian Sea, *J. Phys. Oceanogr.*, 19, 501–519, 1989.
- R. F. Marsden, Physics Department, Royal Roads Military College, FMO Victoria, Victoria, British Columbia, Canada V0S 1B0.
- L. A. Mysak, Climate Research Group, Department of Meteorology, McGill University, 805 Sherbrooke Street West, Montréal, Quebec, Canada H3A 2K6.
- R. A. Myers, Science Branch, Department of Fisheries and Oceans, P.O. Box 5667, St. Johns, Newfoundland, Canada A1C 5X1.

(Received October 10, 1989;  
revised July 18, 1990;  
accepted February 20, 1990.)